DELFT UNIVERSITY OF TECHNOLOGY

FACULTY OF CIVIL ENGINEERING AND GEOSCIENCES

SRON NETHERLANDS INSTITUTE FOR SPACE RESEARCH

MAY 9, 2019

AES4011-10 - ADDITIONAL THESIS

ANALYSIS OF XCO_2 RETRIEVALS FOR CLOUDY OCEAN MEASUREMENTS FROM GOSAT

STUDENT:

BENJAMIN LEUNE (4221125)

SUPERVISORS:

DR. HAILI HU

DR. JOCHEN LANDGRAF

TU Delft Delft University of Technology

SRON Netherlands Institute for Space Research

Preface

During three months, from May until the end of August 2017, I did an internship at the Earth group of SRON in Utrecht. This internship is part of my master program Space Exploration at the Faculty of Aerospace Engineering at the TU Delft, worth 17 EC. At SRON I worked on an academic project of which the details are discussed in this report. Later on I started following a double degree master program by combining my original program with the Geoscience and Remote Sensing master track at the Faculty of Civil Engineering and Geosciences. This internship performed at a research institution also counts towards my degree of that track, in the form of an Additional Thesis (10 EC), as approved by the TU Delft Executive Board.

First, I want to thank Haili for all her support and guidance. Besides teaching me many things, she kept me motivated with her enthusiasm when things did not go as planned. I also want to thank Jochen for the opportunity to do this project and for his useful advice, which helped me to not lose track of the global picture of the project. Finally, I want to thank all the other colleagues and students for the lunch walks and the nice time I have had during my time at SRON.

Contents

Preface i

List of Figures iv

List of Tables v

List of Symbols vi

List of Abbreviations vi

Abstract viii

1 Introduction 1

2 Methodology 4
- 2.1 Data . . . 4
- 2.2 A Priori Filtering . . . 4
- 2.3 Retrieval Algorithm . . . 5
- 2.4 Spatial and Temporal Limits . . . 6
- 2.5 Validation . . . 7
- 2.6 Posterior Filtering . . . 7

3 Results 9
- 3.1 OCO-2 . . . 9
- 3.2 GOSAT . . . 10
  - 3.2.1 Baseline Comparison . . . 10
  - 3.2.2 TCCON Retrieval Comparison . . . 10
  - 3.2.3 Clear-sky Retrieval Comparison . . . 12
  - 3.2.4 Glint Retrieval Comparison . . . 14
  - 3.2.5 Retrieval Statistics . . . 16
  - 3.2.6 Data Yield . . . 17
  - 3.2.7 XCO_2 Maps . . . 19
  - 3.2.8 Cloud Climatology . . . 23

4 Conclusions and Recommendations 26

Bibliography 30

List of Figures

1.1 Schematic overview of a reflected solar SWIR spectrum measurement for a clear-sky land scene. . . . 2
1.2 Schematic overview of the possible light path shortening and lengthening by scattering events in the atmosphere. . . . 3
1.3 Schematic overview of nadir and glint mode observations. . . . 3

2.1 Indicated areas of interest in which retrievals were performed on cloudy GOSAT measurements. . . . 7

3.1 Comparison XCO_2 of TCCON and cloudy retrievals OCO-2. . . . 9
3.2 Comparison XCO_2 of TCCON and GOSAT RemoTeC cloudy retrievals. . . . 11
3.3 Maps indicating locations of colocated TCCON measurements and cloudy retrievals. . . . 12
3.4 Comparison XCO_2 of clear-sky and cloudy retrievals. . . . 13
3.5 Maps indicating locations of colocated clear-sky and cloudy retrievals. . . . 14
3.6 Comparison XCO_2 of glint and cloudy retrievals. . . . 15
3.7 Maps indicating locations of colocated glint and cloudy retrievals. . . . 16
3.8 Data yield comparison between GOSAT cloudy and glint retrievals, North America. . . . 17
3.9 Data yield comparison between GOSAT cloudy and glint retrievals, East Asia. . . . 18
3.10 Data yield comparison between GOSAT cloudy and glint retrievals, South America. . . . 18
3.11 Data yield comparison between GOSAT cloudy and glint retrievals, Oceania. . . . 18
3.12 Data yield comparison between GOSAT cloudy and glint retrievals, Pacific Ocean. . . . 19
3.13 Estimation of the amount of filtered retrievals for cloud ocean, clear-sky and glint per year. . . . 19
3.14 XCO_2 retrieved from cloudy GOSAT measurements in North America. . . . 20
3.15 XCO_2 retrieved from cloudy GOSAT measurements in East Asia. . . . 20
3.16 XCO_2 retrieved from cloudy GOSAT measurements in South America. . . . 21
3.17 XCO_2 retrieved from cloudy GOSAT measurements in Oceania. . . . 21
3.18 ΔXCO_2 retrieved from cloudy GOSAT measurements in Pacific Ocean, 2.0x2.0 deg, 2009-2012. . . . 22
3.19 Timeseries of XCO_2 cloud retrievals, North America. . . . 22
3.20 Timeseries of XCO_2 cloud retrievals, Oceania. . . . 23
3.21 Histograms with the retrieved cloud and aerosol parameters for Oceania. . . . 23
3.22 Histograms with the retrieved cloud and aerosol parameters for East-Asia. . . . 24
3.23 Amount of filtered retrievals as percentage of total retrieval amount for East Asia in 2010-2012. . . . 25
3.24 World maps with cloud climatology with retrieval areas indicated. . . . 25

List of Tables

2.1 A priori values for several state vector element used in the retrieval setup. . . . 6
2.2 Criteria used for posterior filtering of the cloud retrievals. . . . 8

3.1 Overview of statistics of the retrievals and comparisons to TCCON, clear-sky and glint. 17

List of Symbols

Symbol	Explanation	Unit
I	Solar irradiance	W/m^2
N	Number	-
R	Reflectance	W/m^2
r_{eff}	Effective droplet radius	μm
SZA	Solar zenith angle	deg
v_{eff}	Effective droplet radius variance	μm
w_{cloud}	Cloud thickness	m
XCO_2	Column averaged carbon dioxide dry air mole fraction	ppm
z_{cloud}	Cloud height	m
χ^2	Chi squared	-
μ	Arithmetic mean	-
σ	Standard deviation	-
τ_{cloud}	Cloud optical thickness	-

List of Abbreviations

Abbreviation	Explanation
CH_4	Methane
CO	Carbon monoxide
CO_2	Carbon dioxide
ESA	European Space Agency
GOSAT	Greenhouse Gases Observing Satellite
H_2O	Water
ISCCP	International Satellite Cloud Climatology Project
JAXA	Japan Aerospace Exploration Agency
L1B	Level 1B
LER	Lambertian Equivalent Reflectance
NASA	National Aeronautics and Space Administration
NWO	Netherlands Organisation for Scientific Research
OCO-2	Orbiting Carbon Observatory-2
SCIAMACHY	SCanning Imaging Absorption SpectroMeter for Atmospheric CHartographY
SRFP	SRON Full-Physics
SRON	Space Research Organisation Netherlands
SWIR	Short-Wave InfraRed
SZA	Solar Zenith Angle
TANSO-FTS	Thermal and Near infrared Sensor for carbon Observation-Fourier Transform Spectrometer
TCCON	Total Carbon Column Observing Network
XCO_2	Column averaged carbon dioxide dry air mole fraction

Abstract

The atmospheric carbon dioxide (CO_2) concentration has risen from 278 parts per million (ppm) in 1750 to 390.5 ppm in 2011. This increase is caused by anthropogenic emission, predominantly fossil fuel combustion. There is sufficient capacity in the oceans to take up to 70 to 80% of this amount, however, due to the large time scale of this process it can take several hundred years to reach this value. The response of these sinks to a changing climate are important to predict the future behaviour of the carbon cycle with increasing emissions. Space-based observations of column averaged CO_2 dry air mole fraction (XCO_2) with near-global coverage can be used to better quantify the fluxes of small-scale sinks and sources.

The current data set can be significantly extended by performing XCO_2 retrievals for measurements above cloudy ocean scenes as proposed by [Schepers et al., 2016]. This method is based on a full physics retrieval algorithm called RemoTeC, which has been used to retrieve XCO_2 and XCH_4 from GOSAT land and glint measurements. In this study the cloudy retrieval method is performed on a larger scale and an analysis of the data yield and increased spatial coverage of XCO_2 over the oceans is done, a quantitative comparison is made with GOSAT XCO_2 retrievals obtained from TCCON, clear-sky land and glint ocean measurements and the influence of cloud climatology on the retrievals performance is assessed.

The cloudy retrieval was done for GOSAT L1B spectra from measurements obtained between 2009 and 2013 for several areas of interest: North-America, South-America, East-Asia, Oceania and a strip of Pacific Ocean. After a priori filtering for clouds and other parameters, on average 14% of the retrievals gave successful results.

There is a significant increase in data coverage above the oceans, on average 2.4 more cloud retrievals than glint retrievals in areas where both methods can be applied. Furthermore, glint measurements are limited to low and middle latitudes, whereas cloud retrievals can be performed at all measurement latitudes. Extrapolating the results gives an indication of the global data yield, which is approximately 2.5 times higher than the amount of successful clear-sky retrievals and approximately 8 times higher than the amount of glint retrievals per year. However, the quality of the data is poor with a scatter of the error with TCCON measurements of on average 4.23 ppm, compared to 2.50 ppm.

The comparison of the retrieval results with colocated TCCON measurements indicated a geographical dependency, where retrievals from Oceania and North America show significantly robuster statistics than the ones from East Asia. The comparison with colocated clear-sky and glint full physics retrievals show the same pattern, with an average error scatter of respectively 5.00 ppm and 5.03 ppm XCO_2.

The influence of cloud climatology was analysed by looking at correlations between ISCCP cloud data and the retrieval results. The relative high amount and quality of successful retrievals over North-America and Oceania compared to East Asia could have been caused by a higher amount of low liquid clouds above those areas. Another reason could be the larger amount of cirrus cloud situated above South Asia, which also show a seasonal dependency. Further investigation into the influence of cloud climatology using a quantitative approach is necessary.

The quality of the retrieved XCO_2 values are too poor compared to clear-sky and glint retrievals to be of use, however, the significantly higher data coverage makes it seem worthwhile to invest in the cloud retrieval method. In further effort the cloud filter should be revised, which would decrease the amount of non-converging retrievals and thus save computational effort. This would make an analysis of the complete dataset of GOSAT and especially OCO-2 measurements more feasible. A more sophisticated cloud filter that would be able to distinguish undesired difficult cloud scenes from the low liquid clouds would further reduce the computation time and retrieval error.

1 Introduction

The atmospheric carbon dioxide (CO_2) concentration has risen from 278 parts per million (ppm) in 1750 to 390.5 ppm in 2011. This increase is caused by anthropogenic emission, predominantly fossil fuel combustion and in lesser amount cement production and land use change (mainly deforestation) [Stocker, 2014].

However, atmospheric CO_2 is increasing at half of the rate of anthropogenic emissions, the other half is taken up by sinks in the ocean or terrestrial ecosystems. The ocean contains about 50 times more carbon than the atmosphere, and both exchange carbon with a time scale in the order of hundreds of years. There is sufficient capacity in the oceans to take up to 70 to 80% of the anthropogenic emissions, however, due to the large time scale of this process it can take several hundred years to reach this value. Meanwhile the uptake rate of the surface water decreases with increasing atmospheric CO_2 concentration [Prentice et al., 2001]. The response of these sinks to a changing climate are important to predict the future behaviour of the carbon cycle with increasing anthropogenic emissions.

Inverse models estimating the carbon budget on hemispheric scale depend primarily on in situ measurements (flask samples, long term measurement stations) of the CO_2 concentration. On this scale the flux estimates are well known, however, on regional scales large discrepancies still exist due to spatially sparse measurements and boundary layer height and vertical mixing errors in transport models. Space-based observations of column averaged CO_2 dry air mole fraction (XCO_2) with near-global coverage can be used to better quantity the fluxes of small-scale sinks and sources [Eldering et al., 2017].

Earth radiance spectra contain information about the abundance of the trace gases present in the atmosphere. Absorption of the sunlight by the gas molecules occurs at characteristic wavelengths for each species, where the depth of the absorption line is related to the number of molecules of a certain trace gas. In order to do this the length of the effective light path needs to be estimated, where scattering due to aerosols and clouds has to be accounted for. For a schematic overview see Figure 1.1[1] and 1.2.

The Japanese Greenhouse Gases Observing Satellite (GOSAT) was launched in January 2009 with onboard the Thermal and Near infrared Sensor for carbon Observation-Fourier Transform Spectrometer (TANSO-FTS). This instrument measures the spectra of the solar short-wave infrared (SWIR) reflected on the Earths surface and atmosphere and the thermal infrared light emitted by the Earth, however, the latter is not used in this project. The instrument operates by default in nadir observational mode and switches to solar glint observational mode when situated above water in a suitable geometry, see Figure 1.3[2]. It can also operate in target mode, where the instrument is instructed to aim at a point of interest [Kuze et al., 2009].

Improving the current regional flux uncertainties obtained from in site measurements is a challenge for space-based remote sensing, because XCO_2 precisions of 1-2 ppm (0.25-0.50%) are needed to detect the regional sinks and sources against the background level [Miller et al., 2007]. Current regional flux estimates from GOSAT have not produced robust regional flux estimates yet. Fluxes obtained

[1] https://www.nasa.gov/content/orbiting-carbon-observatory-2

[2] https://directory.eoportal.org/web/eoportal/satellite-missions/t/tansat

from combining land and sparsely covered glint ocean XCO_2 retrievals result in more consistent estimates on regional scale [Deng et al., 2016].

However, the current data set can be significantly extended by performing XCO_2 retrievals for measurements above cloudy ocean scenes as proposed by [Schepers et al., 2016]. Due to the ocean's low albedo, the reflection in SWIR is negligible and the backscattered signal comes from the cloud layer. This method is based on a full physics retrieval algorithm called RemoTeC, [Butz et al., 2011], which has been used to retrieve XCO_2 and XCH_4 from GOSAT land and glint measurements [Guerlet et al., 2013], [Alexe et al., 2015], [O'Dell and Feist, 2016]. For RemoTeC to model the light scattering by a optically thick water cloud, a new version of the radiative transfer model is used [Schepers et al., 2014]. Assuming the cloud layer is horizontally homogeneous, fully covering the ground pixel and described by four scattering parameters, a retrieval of XCO_2 can be performed. This method has shown its potential by resulting in XCO_2 average retrieval bias and standard deviation of, respectively, -0.04 ppm and 4.71 ppm, for colocated measurements of several stations of the Total Carbon Column Observing Network (TCCON) [Schepers et al., 2016].

This study aims to perform the cloudy retrieval method on a larger scale and to analyse the data yield and the potentially increased spatial coverage of XCO_2 over the oceans. Also, the performance of the algorithm was tested for measurements of the OCO-2 satellite, which has been launched by NASA in 2014. Furthermore, a quantitative comparison is made with GOSAT XCO_2 retrievals obtained from TCCON, clear-sky land and glint ocean measurements. Finally an analysis is done on the quality of this retrieval method performed on measurements from areas with different cloud climatology.

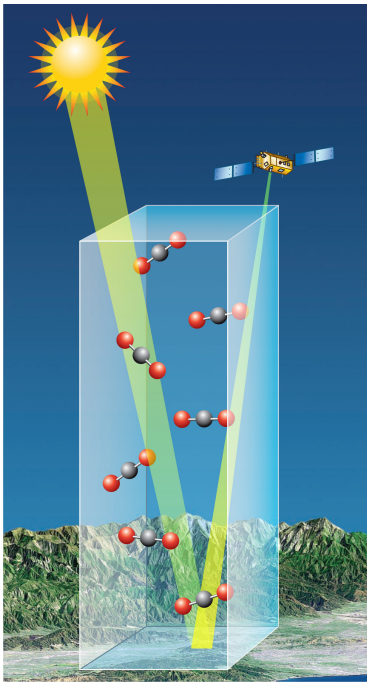

Figure 1.1: Schematic overview of a reflected solar SWIR spectrum measurement for a clear-sky land scene. Source: NASA.[1]

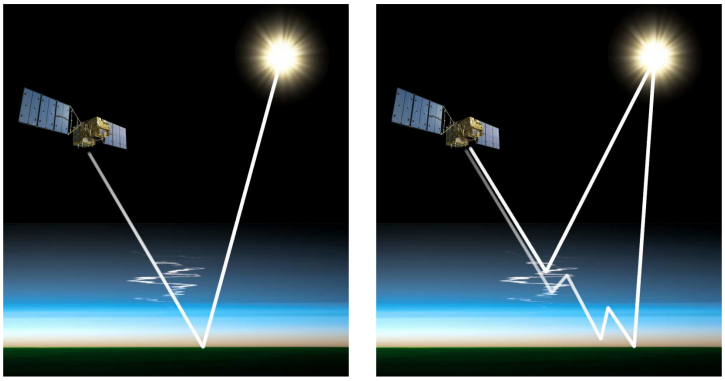

Figure 1.2: Schematic overview of the possible light path shortening and lengthening by scattering events in the atmosphere. Source: [Schepers, 2016].

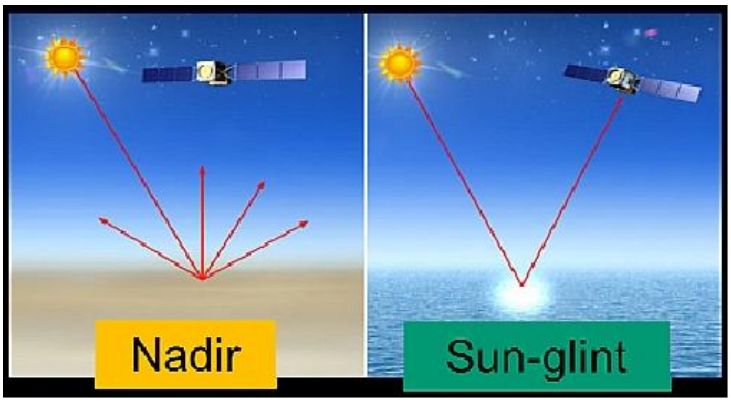

Figure 1.3: Schematic overview of nadir and glint mode observations. Source: TanSat.[2]

2 Methodology

This chapter is describing the data and methods used during this research. First it gives an overview of the data sources used for analysis and validation, after which an insight is given of the criteria used to filter this data. Then the retrieval algorithm is briefly described, followed by the spatial and temporal boundaries of the analysis done. After this the validation method is elaborated on and finally the posterior filers are discussed.

2.1 Data

GOSAT is in a sun-synchronous polar orbit at an altitude of 666 km with a 3-day repeat pattern. Its TANSO-FTS instrument measures sunlight reflected from the Earth's surface and atmosphere in three channels in SWIR, centred at 0.76 μm, 1.60 μm and 2.00 μm, respectively band 1,2 and 3. It has a circular footprint with a diameter of 10.5 km at nadir. The instruments generally operates in nadir mode, only when a suitable geometry is met over water it operates in glint mode, where it measures the specular reflected sunlight by the water in the instruments direction. In the three day cycle TANSO-FTS collects 56000 measurements, however, primarily due to clouds, currently only two to five percent can be used for retrievals.[3] The reason for the low data yield is because the current retrieval algorithms are only applicable to clear-sky land scenes and clear-sky ocean scenes in glint geometry. The cloudy retrievals over ocean has the potential to increase the data yield by approximately a factor 2, considering that 2/3 of the Earth's surface is water and about 80% is cloudy.

For this study Level 1B (L1B) data (version 201) from GOSAT is used, containing calibrated radiance spectral data. The retrieval algorithm needs auxiliary data, such as meteorology, surface elevation and a priori profiles of the absorbing molecules. Preprocessor software resamples this auxiliary data on the satellite footprints. For this project, existing preprocessor files at SRON were used.

In the validation measurements from TCCON were used, a network of inter-calibrated ground based Fourier transform spectrometers recording direct sunlight spectra in the SWIR, providing accurate measurements of atmospheric trace gas abundances, including XCO_2. [De Mazière et al., 2014, Griffith et al., 2014b, Griffith et al., 2014a, Ohyama et al., 2009, Kawakami et al., 2014, Sherlock et al., 2014, Blumenstock et al., 2014, Wennberg et al., 2014a, Wennberg et al., 2014a, Wennberg et al., 2014b]. The GGG2014 version is used.

For further validation, SRON's XCO_2 full-physics RemoTeC retrievals (SRFP) from GOSAT clear-sky and glint measurements were used. All data can be found at the Climate Research Data Package database (`http://www.esa-ghg-cci.org/sites/default/files/documents/public/documents/GHG-CCI_DATA.html`).

2.2 A Priori Filtering

The GOSAT spectra on which a retrieval will be attempted are selected on the following criteria:

[3] Retrieved from: `http://www.gosat.nies.go.jp/eng/gosat/page2.htm`

- Master quality flag - this flag has to indicate that the spectrum is of 'good' quality.
- Glint flag - this selects only the spectra where the measurement mode of the spectrum was nadir pointing and not glint pointing.
- Land flag - the spectrum has to be taken above water, thus neither land or land-water mix.
- Time - the spectrum has to be taken before between 2009 and end 2012 (see Section 2.4).
- Location - the spectrum is filtered on latitude and longitude an has to be taken in the desired area (see Section 2.4).
- Lambertian equivalent reflectance (LER) - when the maximum of this value, calculated with Equation 2.1, exceeds 0.15 in the 1.60 μm window, it is considered to have potentially adequate cloud cover for this retrieval. SZA in this equation stands for the Solar Zenith Angle and R for the measured radiance at a certain spectral value, both obtained from the GOSAT data. I is the solar radiance at the same spectral value as R, obtained from interpolating a reference solar irradiance spectrum.

$$LER(\lambda) = \frac{R(\lambda)}{I(\lambda)} \cdot \frac{\pi}{cos(SZA)} \tag{2.1}$$

When applying the cloud filter, thus having a nadir measurement of good quality above water with a LER above 0.15, to all GOSAT spectra, approximately 30% of the L1B data remains.

2.3 Retrieval Algorithm

The retrieval was performed for the selected GOSAT spectra with the full-physics algorithm RemoTeC v2.4.6 [Butz et al., 2011]. The algorithm consists of an iterative inversion procedure of a forward model relating a state of the atmosphere to the radiance observed by the instrument. In Equation 2.2 the retrieval state vector $\mathbf{x}$ is related to the observation vector $\mathbf{y}$ with the forward model $\mathbf{F}$, where ϵ denotes the measurement and model error [Schepers et al., 2016].

$$\mathbf{y} = \mathbf{F}(\mathbf{x}) + \epsilon \tag{2.2}$$

The inverse algorithm optimizes the state vector $\mathbf{x}$ iteratively by minimizing a least square cost function and a regularization parameter, which is required because the problem is ill-posed.

The RemoTeC full physics algorithm is using a specific setup, where four effective scattering parameters are being retrieved, describing a single-layer, optically thick water cloud [Schepers et al., 2016]. Furthermore, it uses the radiative transfer model LINTRAN V2.1 [Schepers et al., 2014]. The vertical cloud profiles are treated as a Gaussian distributions centred at height z_{cloud} with a full width at half maximum cloud thickness of w_{cloud}. It is assumed the cloud consists of spherical water droplets, where a gamma-distribution as function of the effective droplet radius r_{eff} and variance v_{eff} (fixed to 0.05) describes their size. The four retrieved parameters are: z_{cloud}, w_{cloud}, v_{eff} and the cloud optical thickness τ_{cloud} at 765 nm. The surface albedo is not retrieved and set to zero, as is suitable for ocean surfaces. Table 2.1 denotes several a priori values used for the state vector elements. CO_2 vertical profiles from CarbonTracker 2013 are used, besides as initial guess for the algorithm, to fill up

the null-space below the cloud layer which is not retrieved [Peters et al., 2007]. The null space represents the layers of the atmosphere that the measurements are not sensitive to, in this case primarily the sub-cloud layer.

Table 2.1: A priori values for several state vector element used in the retrieval setup.

State vector element	**A priori value**
CO_2 profile	CarbonTracker 2013
z_{cloud}	1000 m
w_{cloud}	200 m
r_{eff}	12.5 μm
Number density	Derived from τ=15

2.4 Spatial and Temporal Limits

An initial retrieval run of GOSAT measurements colocated with TCCON measurements (see Section 2.5) in the complete time period available (2009 to 2016). There appeared to be a negative bias in the retrieved XCO_2 values compared to the TCCON values, which increased linearly with time in negative direction, starting from 2013. The culprit seemed to be the use of XCO_2 values from CarbonTracker 2013 to fill up the null-space under the retrieved cloud layer, which underestimates the value of XCO_2 because of the 2 ppm/year trend of global CO_2 concentration. With cloud layers situated on average at approximately 1000m, this could significantly alter the retrieved XCO_2 value. Attempts to correct for this trend with a scaling of the a priori CO_2 profiles was not effective. The alternative of rerunning the preprocessor files for GOSAT with CarbonTracker 2016 was not feasible due to time constraints. Instead the analysis was limited to the measurements obtained between 2009 and 2013, mitigating the induced bias.

Initially it was intended to run the retrieval algorithm for GOSAT measurements that were sufficiently cloudy in the above mentioned time period for the entire globe. However, the filter on LER (see Section 2.2) turned out to filter inadequately on difficult cloud cases. This lead to a convergence of the algorithm for on average 44% of the spectra, and only 14% passing the posterior filtering. Non-convergence as a filter for difficult cloud scenarios wastes a significant amount of computation time, since up to 30 iterations are done using a relative large number of layers, trying to resolve an optically thick cloud. Due to the time limitation of 3 months of the research project, it was decided to limit the retrievals to specific areas on the globe to reduce computation time. For illustration, the global dataset between 2009 and 2012 would take 6 weeks using 100 CPU cores. The areas were selected on available TCCON, glint and clear-sky measurements in the vicinity. Furthermore, one area with a large latitudinal range was put over the Pacific Ocean to see if the latitudinal gradient of XCO_2 would be visible. Besides that, it would be interesting to see how the retrievals would behave for the open ocean and to compare the amount of retrievals with glint retrievals for a low latitudinal area. Oceania and Japan were targeted because they had respectively, the best and worst retrieval quality, as compared to TCCON stations in [Schepers et al., 2016]. These areas are indicated as 'boxes' in Figure 2.1.

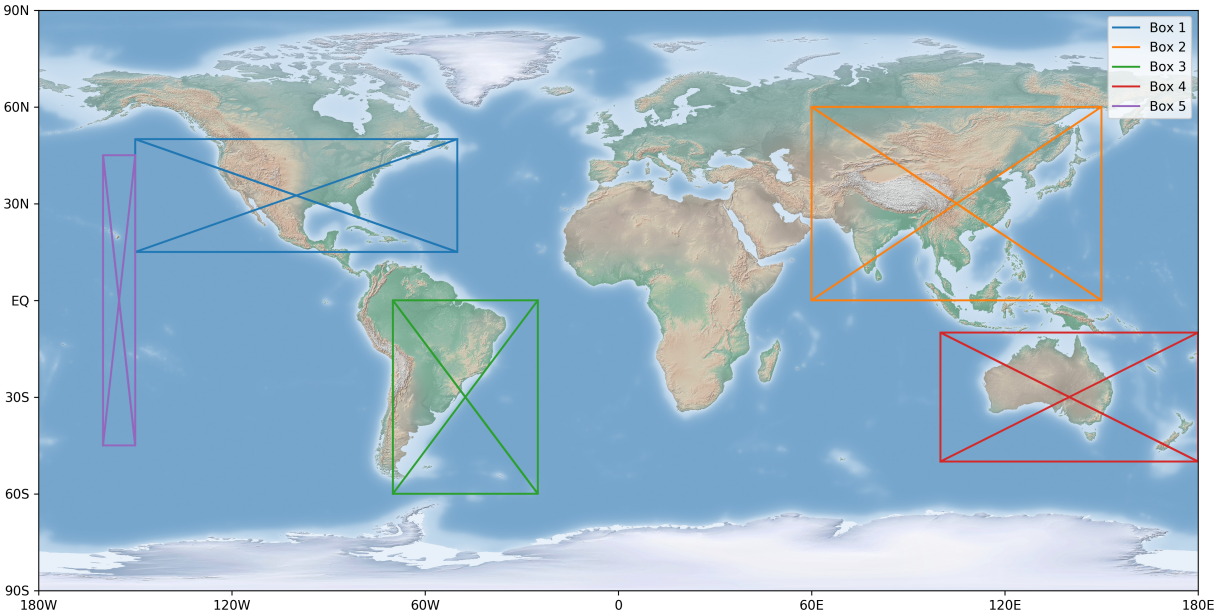

Figure 2.1: Indicated areas of interest in which retrievals were performed on cloudy GOSAT measurements.

2.5 Validation

Validation is performed by comparing the mean and standard deviation of the difference in XCO_2 values from spatially and temporally colocated TCCON measurements and glint and clear-sky full physics retrievals obtained from RemoTeC (SRFP). They were considered colocated if they were taken within 2 hours and within 5 degree central latitudinal and longitudinal difference of each other. Some areas do not appear in the comparisons, because there were not colocations in that area with the comparison data. In the assessment of the quality of the retrievals, one of the key number is the standard deviation of the error, which indicates the scattering of the retrieval. The mean of the error, the bias, is of less importance since a bias correction is typically applied to satellite retrievals.

2.6 Posterior Filtering

During the retrieval process more than half of the retrievals are filtered out, based on non-convergence. Non-convergence is a valid filter for measurements containing difficult cloud scenarios, such as high or vertically structured and irregular clouds, according to [Schepers et al., 2016].

The criteria used for posterior filtering are shown in Table 2.2. These criteria were found by iteration, where their effect on the amount of filtered retrievals and retrieval error were taking into account. The retrieved XCO_2 values were compared to values from colocated clear-sky retrievals, since that was the largest colocated dataset for validation. The error was plotted as function of the retrieved parameters, to spot any trends or other correlations. Applied to the dataset, the filter gave a slightly lower standard deviation of the error, while a larger amount of retrievals passed compared to the filter proposed in [Schepers et al., 2016].

Table 2.2: Criteria used for posterior filtering of the cloud retrievals.

Variable	**Lower boundary**	**Upper boundary**	**Unit**
χ^2 fit	0	8	-
XCO_2 1-σ error	0	1.3	ppm
τ_{cloud}	0	20	-
r_{eff}	0	35	μm
z_{cloud}	-500	1400	m
w_{cloud}	0	1400	m

3 Results

First the results of the cloud retrieval method applied to data from a different satellite will be presented. This work is not included in the other chapters, however the results could still be of interest. Subsequently the results and findings of the GOSAT cloud retrievals are discussed.

3.1 OCO-2

In the beginning of this study, the cloudy retrieval method was tested on data from the Orbiting Carbon Observatory-2 (OCO-2) instrument. OCO-2 has a significantly higher spatial resolution and higher data volume of its measurements than GOSAT. However, it turned out the retrieval algorithm for clouds used for GOSAT applied on OCO-2 resulted in poor quality retrievals compared to the GOSAT cloudy retrievals. In Figure 3.1 a comparison (analogous to the GOSAT comparisons in Section 2.5) is shown between the XCO_2 of the cloudy OCO-2 retrievals and colocated TCCON measurements. Heavy posterior filtering had to be applied to achieve a standard deviation of the error of the same order as GOSAT (see Table 3.1). Of the 46979 retrievals only 9% converged and 2.2% passed the filters, while still having a significant bias. This low data yield resulted in large processing times to reach a adequate amount of retrievals to apply meaningful statistics. The cloud retrieval method in [Schepers et al., 2016] was optimized for GOSAT measurements and requires a large effort to be adjusted correctly for OCO-2. It was then decided to focus on solely GOSAT cloud retrievals.

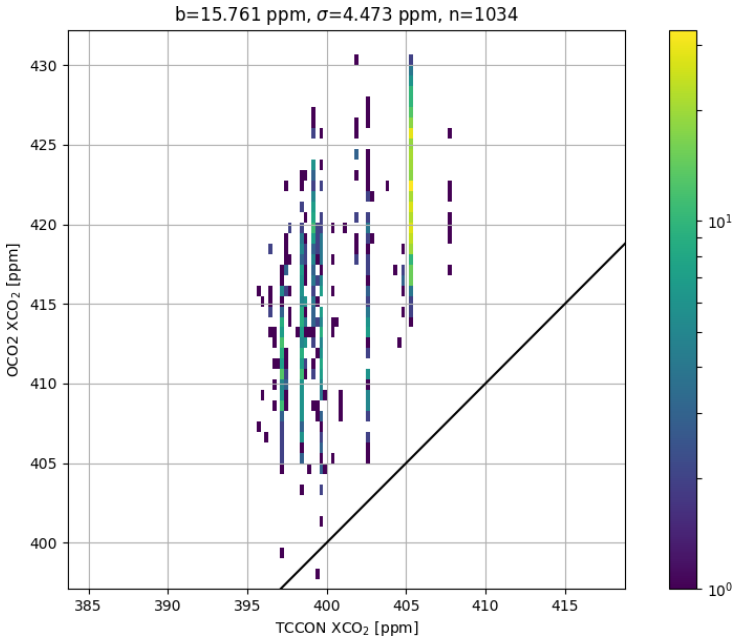

Figure 3.1: Comparison XCO_2 of TCCON and cloudy retrievals OCO-2.

3.2 GOSAT

The retrieval results for the cloudy measurements from GOSAT in the time period of 2009-2012 for the different areas will be discussed here. First a baseline comparison with the results from [Schepers et al., 2016] is drawn. Next, the results from comparing the cloud retrievals to TCCON, glint and clear-sky data are shown followed by an overview of the retrieval statistic. Then the potential increase of data coverage of the cloudy retrievals is analysed. Afterwards, the XCO_2 values are presented and their quality is discussed. Finally, a preliminary analysis is done on the possible correlation between cloud climatology and the differences in retrieval behaviour seen in the different areas.

3.2.1 Baseline Comparison

To verify the used cloudy retrieval method a comparison was done with the XCO_2 errors in [Schepers et al., 2016] resulting from a TCCON validation. The validation was reconstructed with the same eight TCCON stations (Izaña, Caltech, Tsukuba, Ascension, Darwin, Reunion, Wollongong and Lauder) in same time period (April 2009 until December 2013), using the same method to TCCON altitude correction and a priori correction. This resulted in a bias of -2.76 and a standard deviation of the error of 4.91, compared to -0.04 and 4.71 in [Schepers et al., 2016]. Possible causes for the difference in bias can be the different versions of RemoTeC and GOSAT L1B data product that were used. However, the standard deviation of the error is in the same order of magnitude, which is a more valid indicator of the quality of the retrievals than the bias, thus it was decided to continue with the current version of the retrieval algorithm.

3.2.2 TCCON Retrieval Comparison

In the correlation plots in Figure 3.2 the retrieved XCO_2 values of the cloudy GOSAT measurements are plotted as function of their colocated TCCON measurement. In these plots the mean and standard deviation of the difference between the two are indicated, as well as the number of colocations. The points are color coded on a log scale for visibility. Posterior filters are applied to the data, explained in Section 2.6. The standard deviation of both North America and Oceania are in the same order of magnitude as in [Schepers et al., 2016], see Table 3.1. In Figure 3.3 the areas are shown with the position of the cloud retrievals and the TCCON station indicated. The map depicting North America, appears to indicate cloud retrievals were performed on land, however, this is in fact Lake Michigan and other surrounding lakes. In East Asia the TCCON stations shown are from left to right: Saga and Tsukuba, both in Japan. For North America, from left to right: Caltech and Park falls, both in the USA. For Oceania, from left to right: Darwin and Wollongong (both Australia) and Lauder (New Zealand).

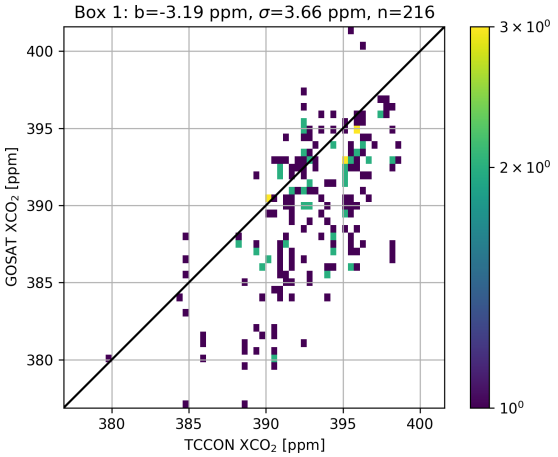

(a) Box 1, North America.

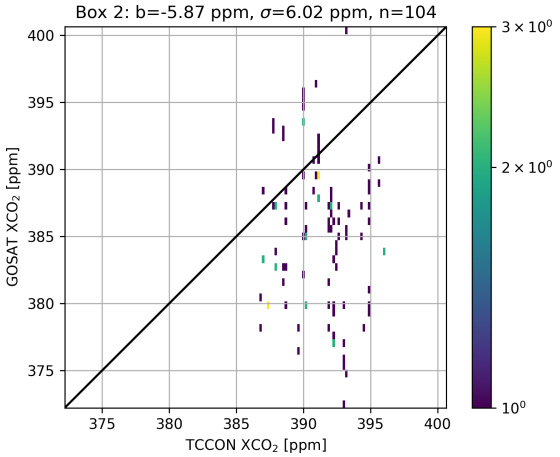

(b) Box 2, East Asia.

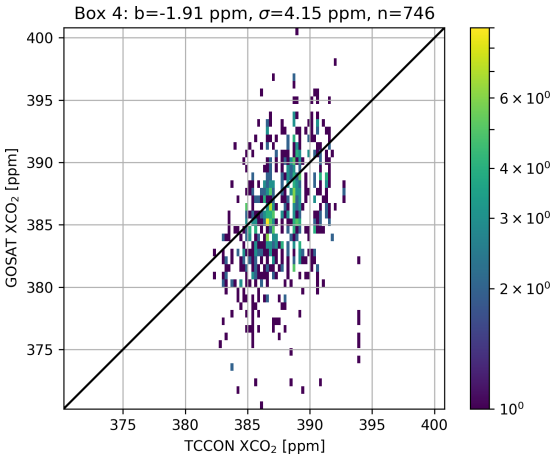

(c) Box 4, Oceania.

Figure 3.2: Comparison XCO_2 of TCCON and GOSAT RemoTeC cloudy retrievals.

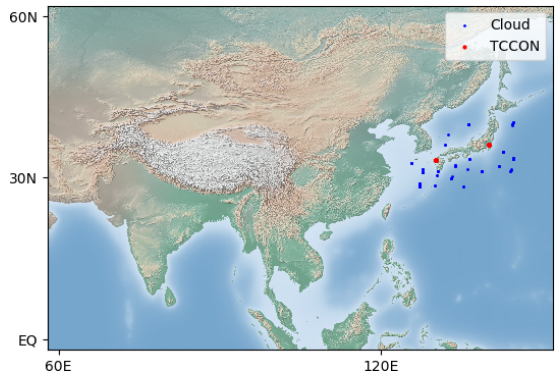

(a) Box 2, East Asia.

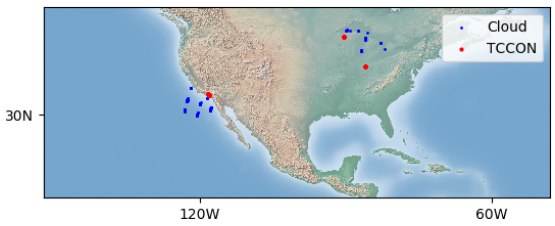

(b) Box 1, North America.

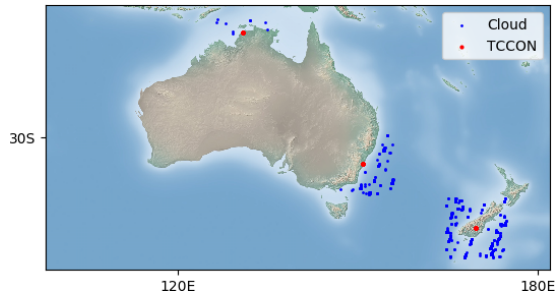

(c) Box 4, Oceania.

Figure 3.3: Maps indicating locations of colocated TCCON measurements and cloudy retrievals.

3.2.3 Clear-sky Retrieval Comparison

In Figure 3.4 the correlation plots are shown for the clearsky retrievals, analogical to the TCCON ones. As can be seen in both the correlation plots as the maps in Figure 3.5, South America and East Asia have significantly less colocations due to less successful cloud retrievals, as explained in Section 3.2. Oceana shows again the best statistics, followed by North America.

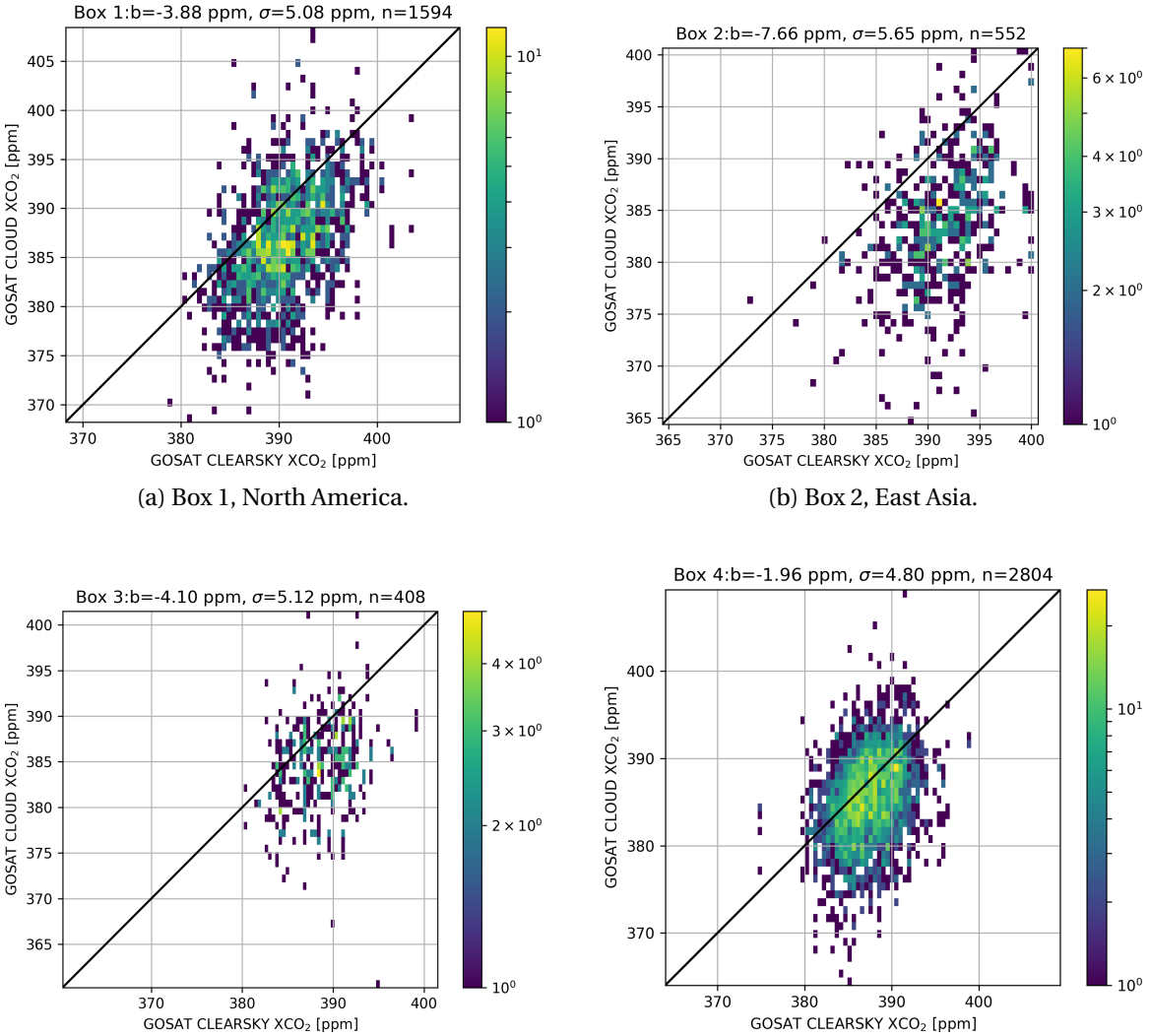

(a) Box 1, North America.

(b) Box 2, East Asia.

(c) Box 3, South America.

(d) Box 4, Oceania.

Figure 3.4: Comparison XCO_2 of clear-sky and cloudy retrievals.

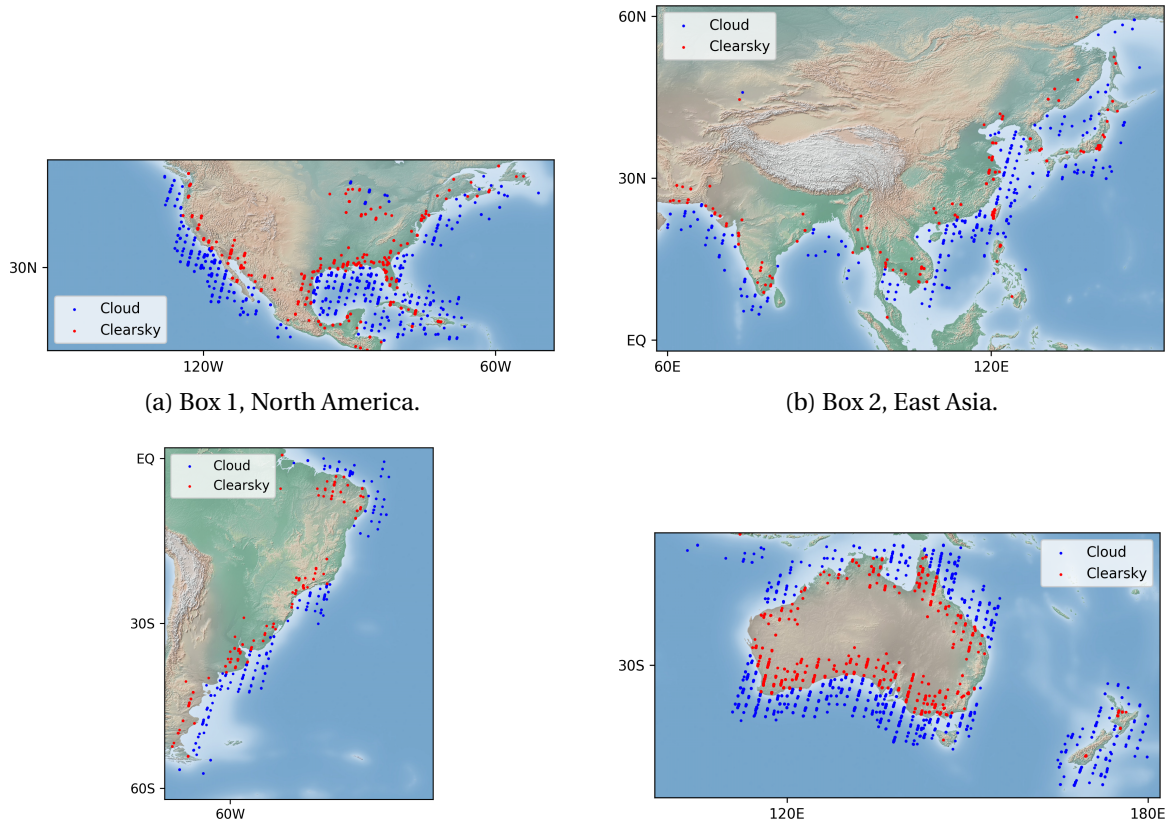

(a) Box 1, North America.

(b) Box 2, East Asia.

(c) Box 3, South America.

(d) Box 4, Oceania.

Figure 3.5: Maps indicating locations of colocated clear-sky and cloudy retrievals.

3.2.4 Glint Retrieval Comparison

Finally, in Figure 3.6 and Figure 3.7 the correlation plots and maps are shown for the colocated glint retrievals. The number of colocations with the glint retrievals are lower than the number of clear-sky colocations, simply because there are less glint retrievals available due to the specific geometry required for a glint measurement. The shown statistics are all in the same range, approximately the same order of magnitude as the clear-sky statistics. The correlation plots seem to be more scattered, however, this is due to the lower number of colocations.

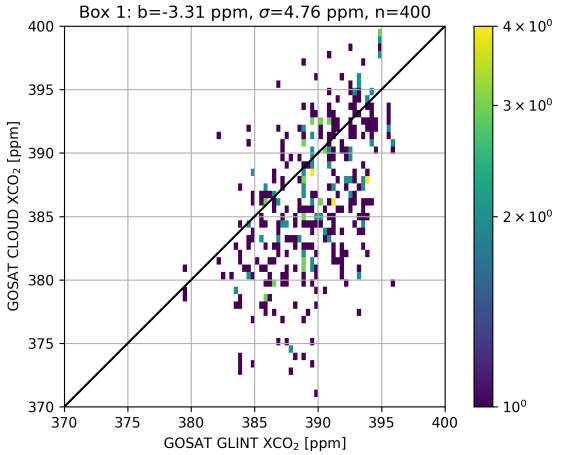

(a) Box 1, North America.

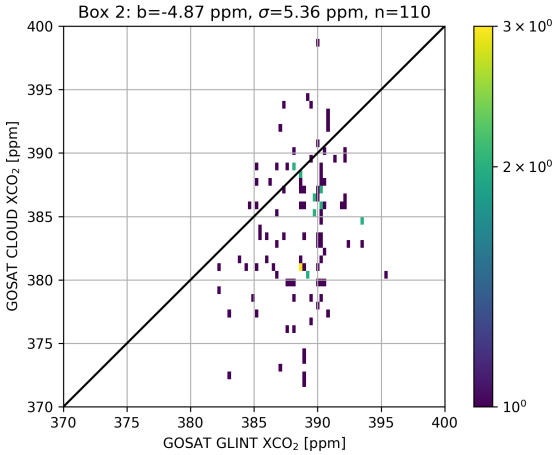

(b) Box 2, East Asia.

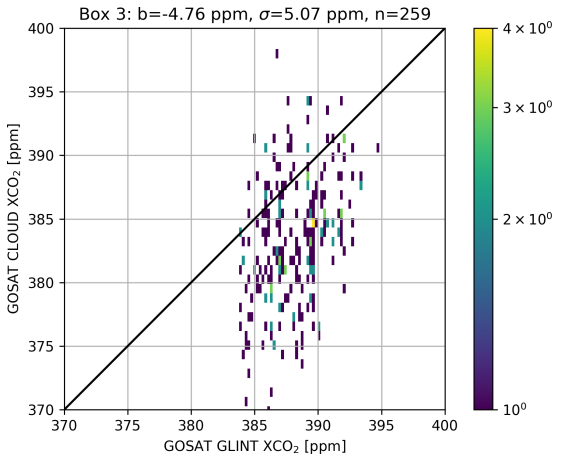

(c) Box 3, South America.

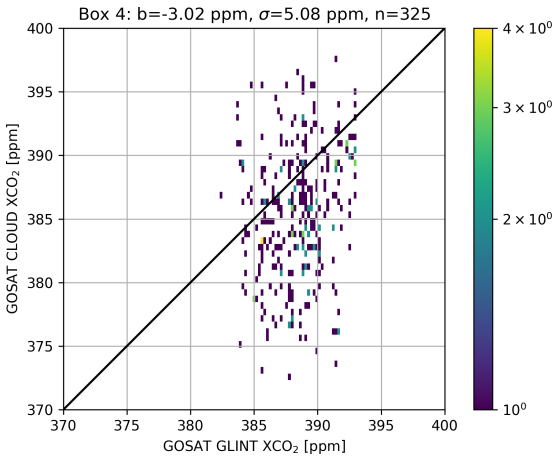

(d) Box 4, Oceania.

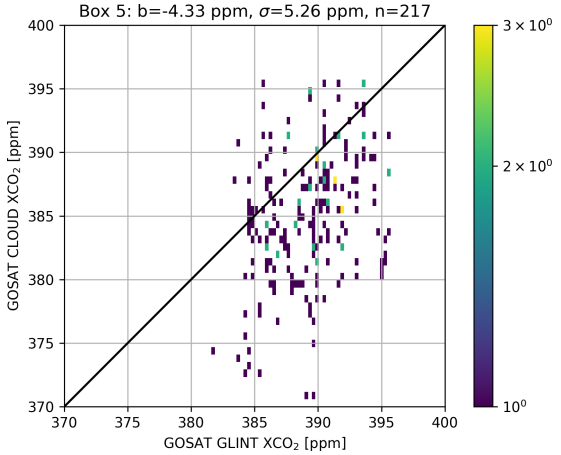

(e) Box 5, Pacific Ocean.

Figure 3.6: Comparison XCO_2 of glint and cloudy retrievals.

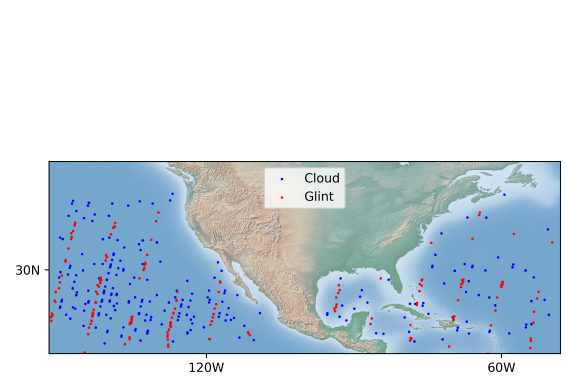

(a) Box 1, North America

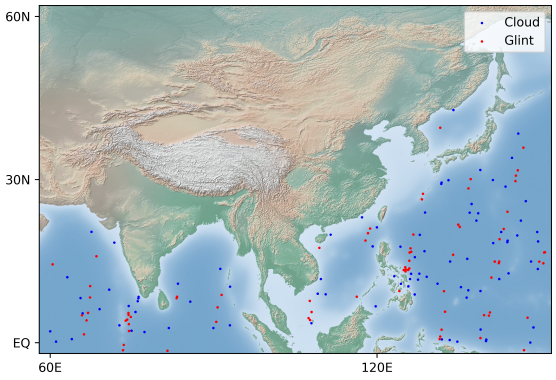

(b) Box 2, East Asia.

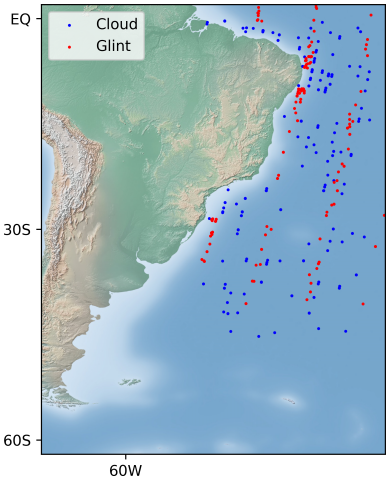

(c) Box 3, South America.

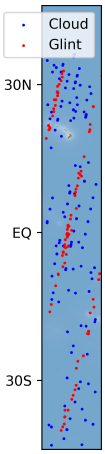

(d) Box 5, Pacific Ocean.

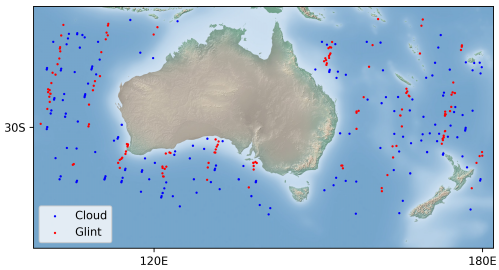

(e) Box 4, Oceania.

Figure 3.7: Maps indicating locations of colocated glint and cloudy retrievals.

3.2.5 Retrieval Statistics

In Table 3.1 several statistics are shown of the retrievals itself and of the comparison with TCCON, clear-sky and glint retrievals. Furthermore several statistics from [Schepers et al., 2016] are taken as comparison. The 'Filtered' value shows the amount of retrievals that passed the posterior filters as percentage of the total number of retrievals. This value is on average 14%, which is significantly lower than the 39% in [Schepers et al., 2016]. A difference in the incorporation of the a priori cloud filter could have caused this, however, this remains unknown, see also Section 2.4. It should be noted that the posterior filters used here differ from the ones in [Schepers et al., 2016] and filter out less retrievals while resulting in a lower standard deviation of the error, as explained in 2.6. The variation in both number of retrievals that passes posterior filtering and colocated error scatter from area to area is significant and indicates there is a certain underlying factor causing this. This will be elaborated on in Section 3.2.8. The quality of the cloud retrievals is relatively bad, compared to the colocated clear-sky and glint retrievals. However, as will be discussed in Section 3.2.6, there is a significant increase in data yield compared to glint measurements. For comparison, the GOSAT XCO_2 data product (SRFP) that was used for validation has a bias and σ of ,respectively, -2.0 and 1.9 ppm, for clear-sky retrievals and -3.2 and 1.3 ppm, respectively, for glint retrievals. The bias is in the same order of magnitude, however, the σ is two to three times as high.

Table 3.1: Overview of statistics of the retrievals and comparisons to TCCON, clear-sky and glint.

	N			TCCON			Clear-sky			Glint		
	Total	Converged [%]	Filtered [%]	N	μ [ppm]	σ [ppm]	N	μ [ppm]	σ [ppm]	N	μ [ppm]	σ [ppm]
North America	165759	50	18	216	-3.19	3.66	1594	-3.88	5.08	400	-3.31	4.76
East Asia	140293	32	6	104	-5.87	6.02	552	-7.66	5.65	110	-4.87	5.36
South America	155265	42	12	0	-	-	408	-4.10	5.12	259	-4.76	5.07
Oceania	196142	50	16	746	-1.91	4.15	2804	-1.96	4.80	325	-3.02	5.08
Pacific Ocean	60289	47	16	0	-	-	0	-	-	217	-4.33	5.26
Total	717748	44	14	1066	-2.56	4.23	5358	-3.28	5.00	1311	-3.82	5.03
[Schepers et al., 2016]	11837	-	39	1423	-0.04	4.71						

3.2.6 Data Yield

One of the reason to perform the retrievals on cloudy measurement above the ocean, was to increase the data amount and spatial-temporal coverage of the data over the ocean. In Figure 3.8 to 3.12, maps are shown depicting the locations of the filtered cloud and glint retrievals in those areas, between 2009 and 2013. The amount of cloud retrievals is around 2.4 times higher than the amount of glint retrievals for an area containing glint retrievals. Furthermore, the geometrical spread of the cloud retrievals is higher than the glint retrievals, which are concentrated on specific locations due to the required geometry for a specular reflection to occur in the direction of the instrument. Besides, the glint retrievals are limited to low and middle latitudes, whereas the cloud retrievals are not, as visible on the maps. The scatter of the error of the cloud retrievals is higher than the one of the glint retrievals, which are approximately 2.50 ppm, compared to TCCON measurements [O'Dell and Feist, 2016].

When extrapolating the filtered retrieval percentage of 14% for the retrieval areas (see Section 3.1) to the global dataset, a rough indication can be made on the amount of filtered retrievals. The amount of yearly filtered retrievals for cloudy ocean, clear-sky and glint measurements are indicated in Figure 3.13. The amount of cloudy ocean retrievals is about 2.5 times the amount of clear-sky retrievals and about 8 times higher than the amount of glint ocean retrievals. However, as mentioned in Section 3.2.5, the quality of the cloud retrieval does not have the same level of quality as the clear-sky and glint retrieval.

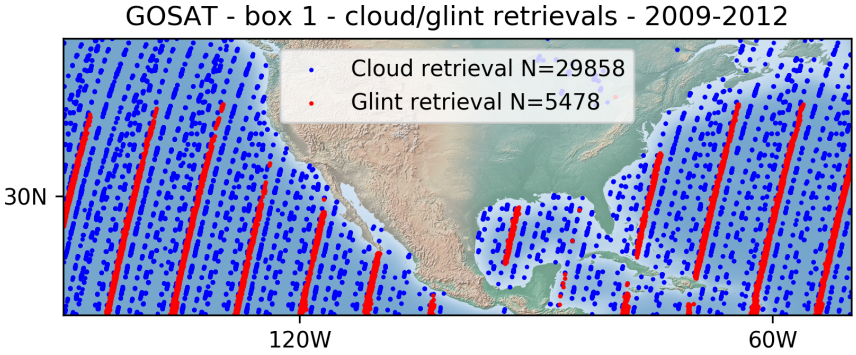

Figure 3.8: Data yield comparison between GOSAT cloudy and glint retrievals, North America.

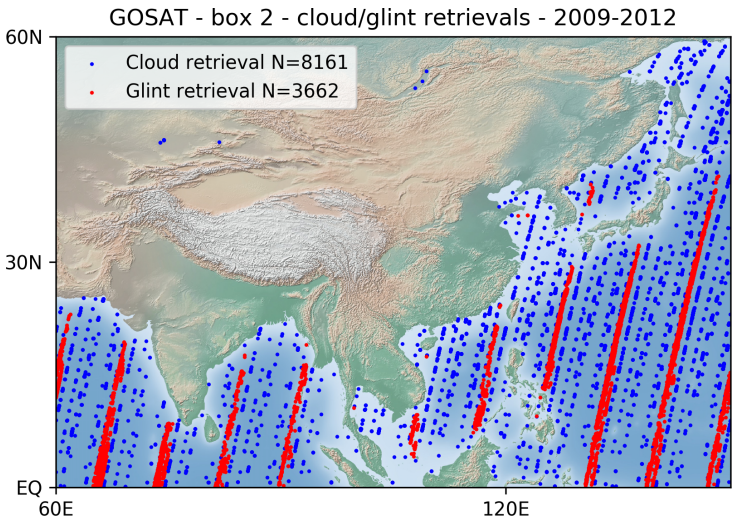

Figure 3.9: Data yield comparison between GOSAT cloudy and glint retrievals, East Asia.

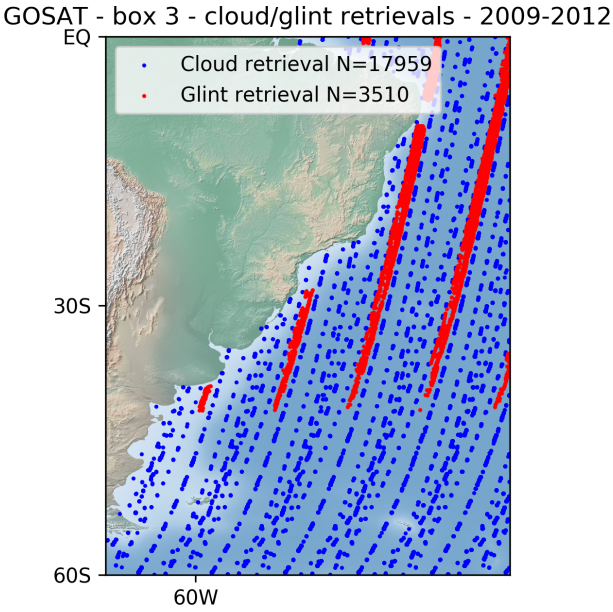

Figure 3.10: Data yield comparison between GOSAT cloudy and glint retrievals, South America.

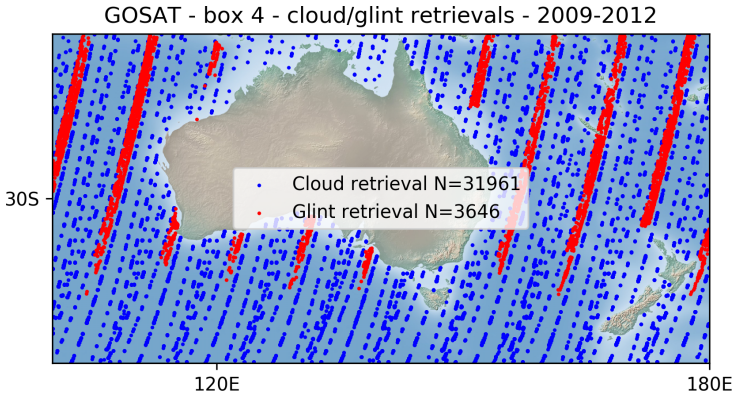

Figure 3.11: Data yield comparison between GOSAT cloudy and glint retrievals, Oceania.

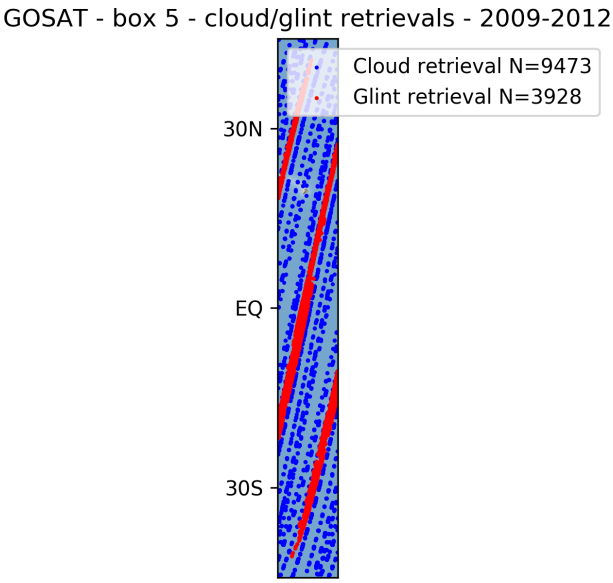

Figure 3.12: Data yield comparison between GOSAT cloudy and glint retrievals, Pacific Ocean.

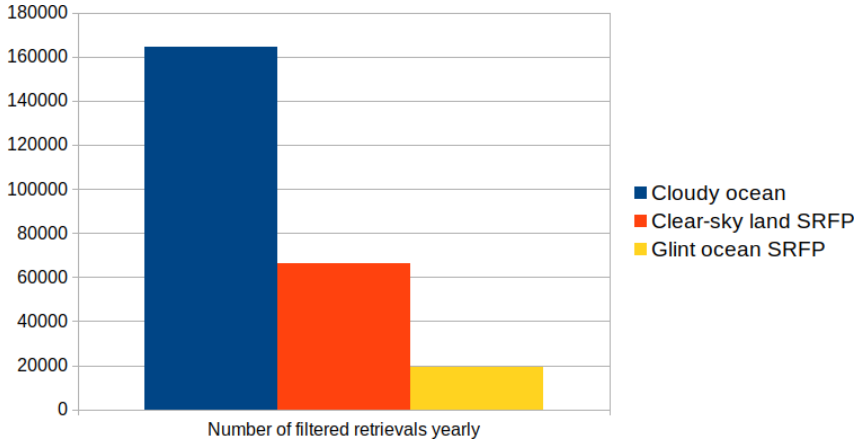

Figure 3.13: Estimation of the amount of filtered retrievals for cloud ocean, clear-sky and glint per year.

3.2.7 XCO_2 Maps

The XCO_2 values obtained from the cloud retrievals for North America, East Asia, South America and Oceania are shown in Figures 3.14 to 3.17, respectively. These retrievals are filtered as described in Section 2.6 and the average value is plotted on 1 degree latitude by 1 degree longitude boxes. The average is weighted with the one-sigma error, as retrieved by the RemoTeC algorithm. The colour map is scaled to have a range from minus one-sigma to plus one-sigma above and below the mean value of XCO_2 in that area for visibility. The variation in number of filtered retrievals, which can be found in Table 3.1, is visible on these maps by looking at the amount of white boxes, where no data is available. The quality of the data is too poor, i.e. the XCO_2 values have significant scatter, at this moment to be able to identify the expected outflow over the ocean from point sources. Furthermore, the quality is adequate enough to be deemed worthy of performing a bias correction.

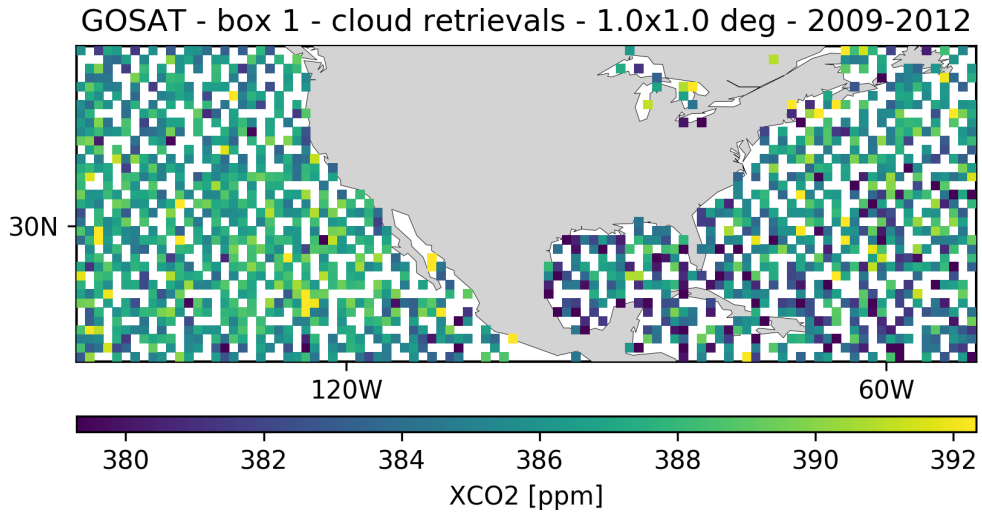

Figure 3.14: XCO_2 retrieved from cloudy GOSAT measurements in North America.

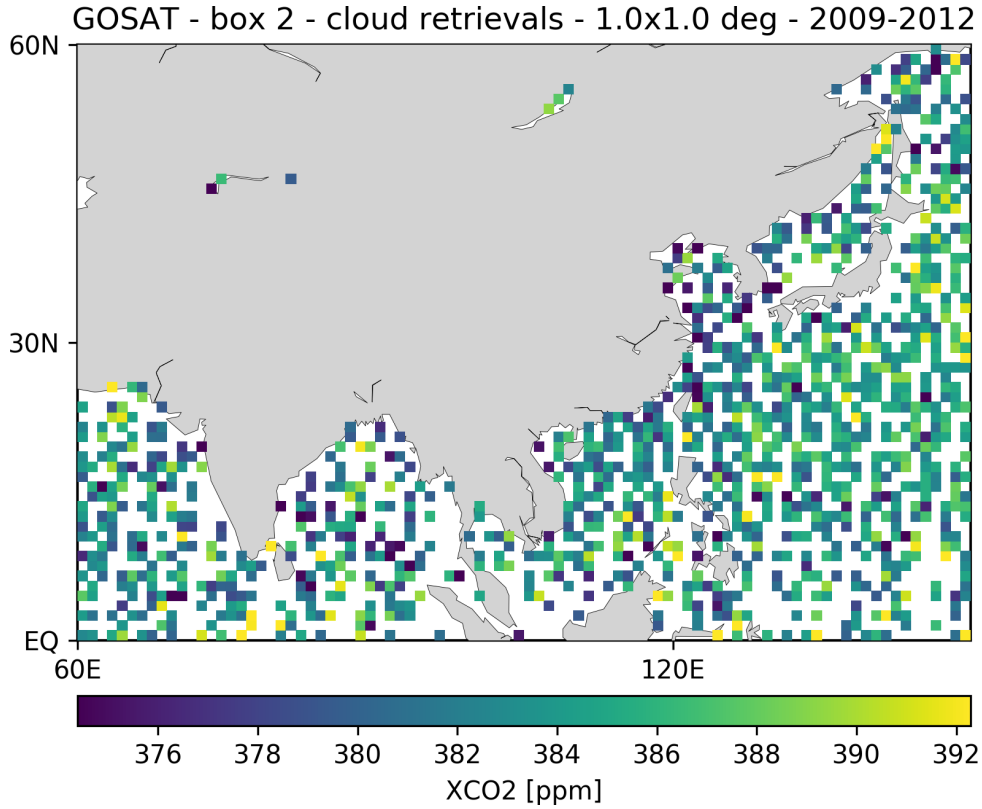

Figure 3.15: XCO_2 retrieved from cloudy GOSAT measurements in East Asia.

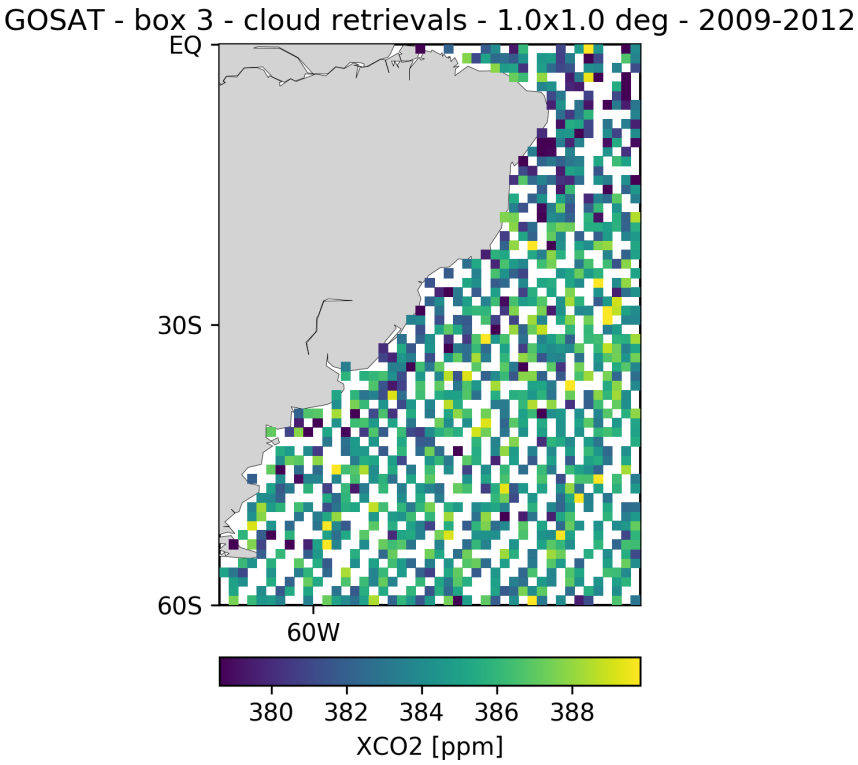

Figure 3.16: XCO_2 retrieved from cloudy GOSAT measurements in South America.

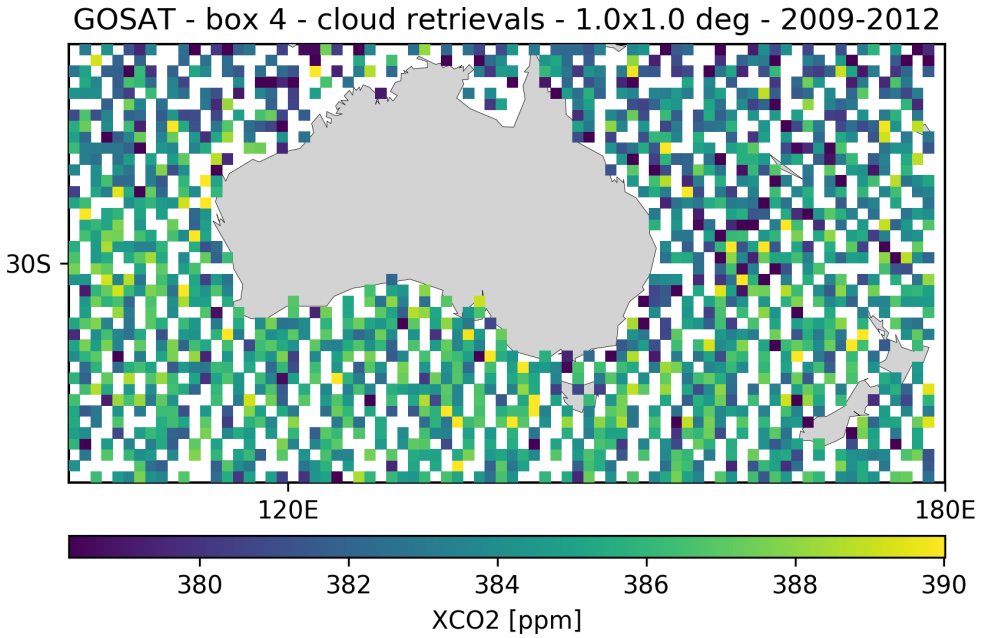

Figure 3.17: XCO_2 retrieved from cloudy GOSAT measurements in Oceania.

For the area in the Pacific Ocean a similar figure is shown in Figure 3.18, where the deviation from the mean is plotted on 2x2 degree boxes. To increase the visibility of the latitudinal gradient of atmospheric CO_2 concentration, the yearly trend and seasonality on the northern hemisphere are removed. A gradient of around 2 ppm from North to South is visible, except for a deviation in the vicinity of the equator, where the retrievals are of less quality (see Section 3.2.8)

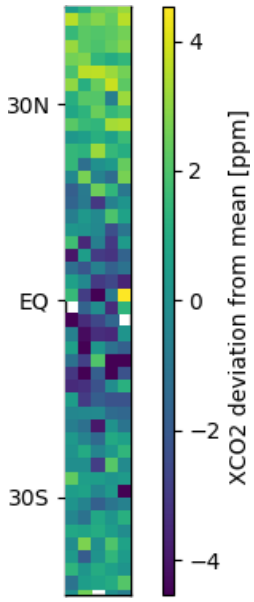

Figure 3.18: ΔXCO_2 retrieved from cloudy GOSAT measurements in Pacific Ocean, 2.0x2.0 deg, 2009-2012.

In Figure 3.19 and 3.20 time series are shown of the XCO_2 values retrieved from the GOSAT measurements in North America and Oceania, respectively. In both series a trend can be seen, with a value of 1.74 and 1.80 ppm per year, which is in the same order of magnitude as the global trend of atmospheric CO_2 concentration. There is no clear seasonality of the XCO_2 in Oceania, while there is significant seasonality in North-America. This corresponds with the relative high seasonality on the northern hemisphere and relative low seasonality on the southern hemisphere of the atmospheric CO_2 concentration.

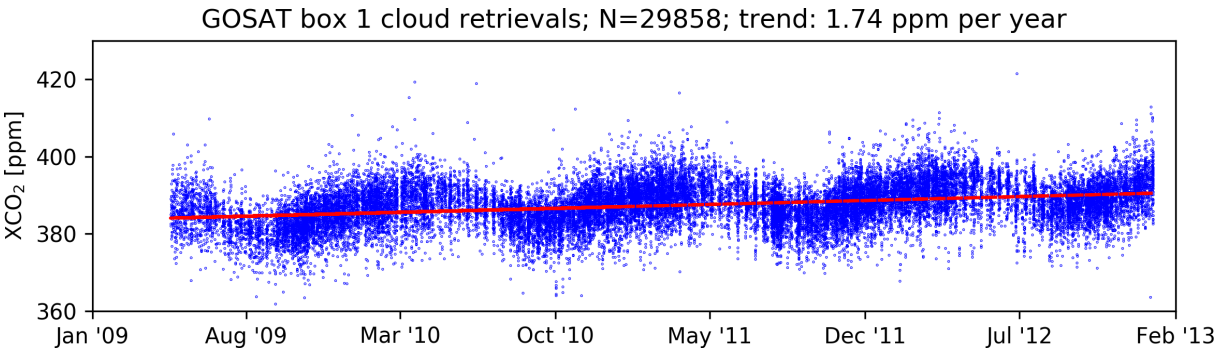

Figure 3.19: Timeseries of XCO_2 cloud retrievals, North America.

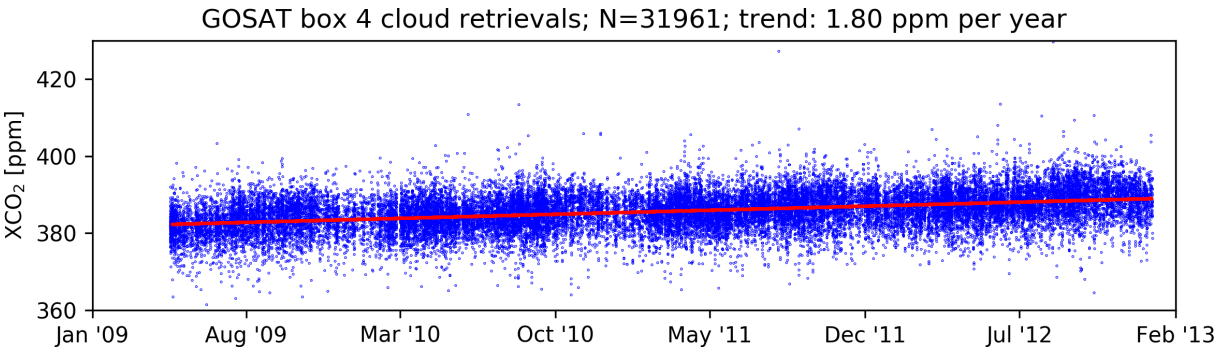

Figure 3.20: Timeseries of XCO_2 cloud retrievals, Oceania.

3.2.8 Cloud Climatology

When comparing the different areas there is a significant difference in the amount of successful (converged and filtered) retrievals and colocation statistics (see Table 3.1). The most striking difference is between North America and Oceania and East Asia. [Schepers et al., 2016] found that retrievals colocated with the TCCON station at Lauder, New Zealand had the best performance, whereas the ones colocated with Tsukuba, Japan has the worst quality. It that study several causes were mentioned, one being the difference in cloud climatology from area to area. Several observations on these possible difference will be discussed.

First the retrieved cloud parameters from the different areas were compared, however, no significant difference was found and the parameters were more or less the same for all areas. In Figure 3.21 and 3.22 histograms are shown of the retrieved cloud parameters (see Section 2.3) for Oceania and East-Asia. Subsequently, the aerosols retrieved in the colocated clear-sky retrievals were looked into. In the cloud setup of the retrieval algorithm, aerosols are not taking into account, which means they could cause a deviation if there is a variability between the areas. The comparison did not show any variability large enough to cause these differences. In Figure 3.21 and 3.22 the histograms of the retrieved aerosol parameters are shown of colocated clear-sky retrievals for Oceania and East-Asia.

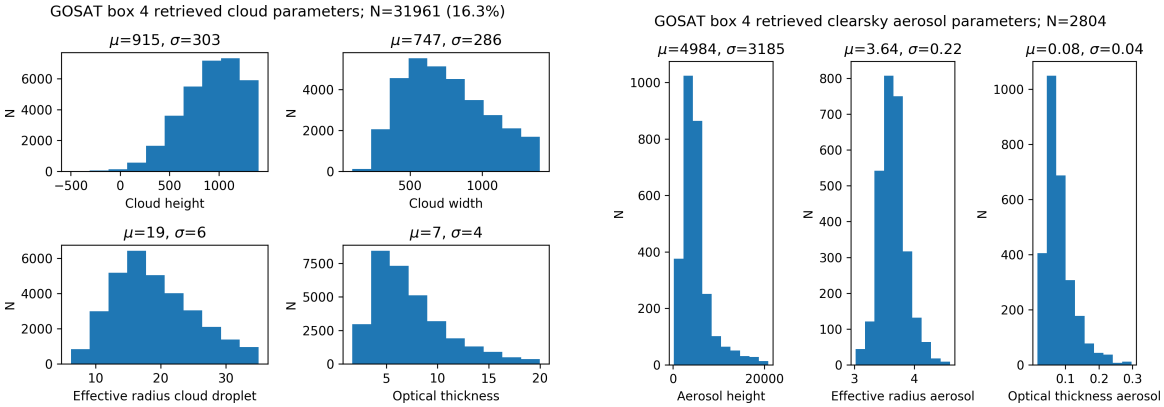

Figure 3.21: Histograms with the retrieved cloud and aerosol parameters for Oceania.

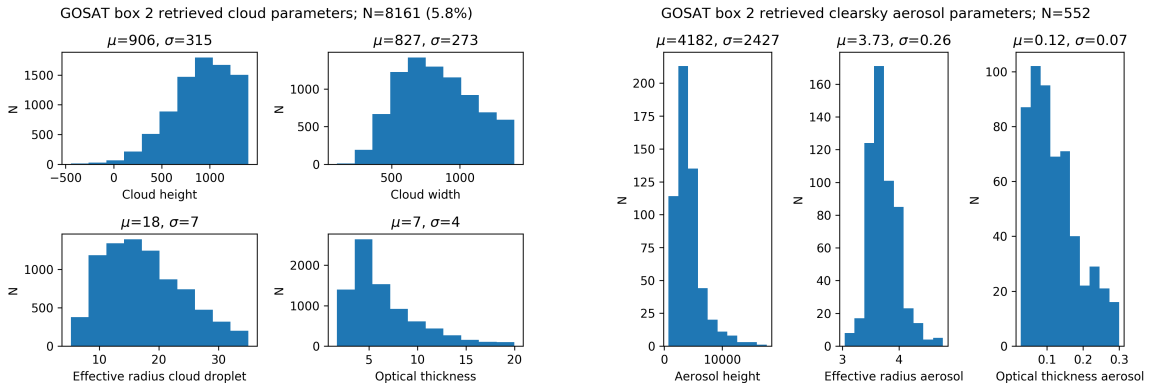

Figure 3.22: Histograms with the retrieved cloud and aerosol parameters for East-Asia.

Cloud climatologies were compared qualitatively for the different areas using the International Satellite Cloud Climatology Project (ISCCP) D2 data [Schiffer and Rossow, 1983], [Rossow and Schiffer, 1999]. First the daytime annual low liquid cloud amounts were compared, since this is the target cloud of the cloud retrieval method used from [Schepers et al., 2016]. In Figure 3.24a there seems to be a possible correlation between the amount of low liquid cloud and the filtered percentage for the different areas (see Table 3.1). For example, North America and Oceania have significantly more annually low liquid clouds compared to East Asia, with respectively 18, 16, 6% filtered retrievals.

Furthermore, in East Asia there is a relative large amount of cirrus clouds, especially in the south, as shown in Figure 3.24b. Measurements containing clouds are known to have a negative effect on retrieval performance, and are often being filtered out. Cirrus clouds cause scattering that can introduce an error of several percent in XCO_2 [Guerlet et al., 2013]. In the Pacific Ocean retrieval area XCO_2, as shown in Figure 3.18, the quality of the retrievals around the equator is poor compared to retrievals with higher/lower latitudes. This corresponds to the increase of cirrus clouds around the equator, as seen in Figure 3.24b. Finally the seasonality of the retrieval quality is compared to the seasonality of cirrus cloud amount shown in Figure 3.24c and 3.24d. The seasonality seen in percentage of filtered retrievals is the most visible in East Asia, as shown in Figure 3.23. In December, January and February the percentage is three times higher than in June, July and August, which corresponds with the cirrus cloud amount seasonality. It should be noted that these apparent correlations might have a different cause than the ones mentioned, since a purely visual comparison was done.

In [Guerlet et al., 2013] a cirrus filter is tested for GOSAT, which looks at the radiance in strong H_2O absorption bands. Due to the scattering by cirrus clouds, the absorption by water vapour can only occur above the cirrus clouds, while for clear-sky cases this is done by the whole atmosphere. If this filter can be applied to measurements containing clouds is unknown, since the lower layer, containing most of the water vapour is blocked. A different cloud filter, which could be applied to remove cirrus contamination is described in [Taylor et al., 2016], where for a non-scattering retrieval the ratio between H_2O in two bands can indicate cloud contamination. Further research is necessary on this topic.

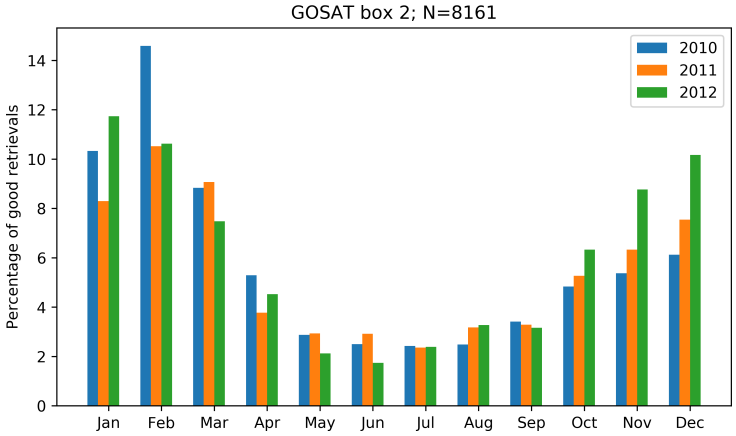

Figure 3.23: Amount of filtered retrievals as percentage of total retrieval amount for East Asia in 2010-2012.

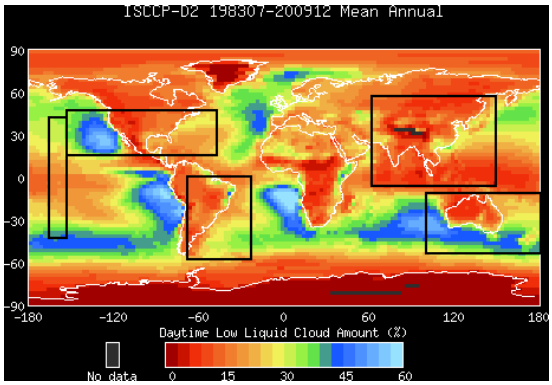

(a) Annual low liquid cloud amount.

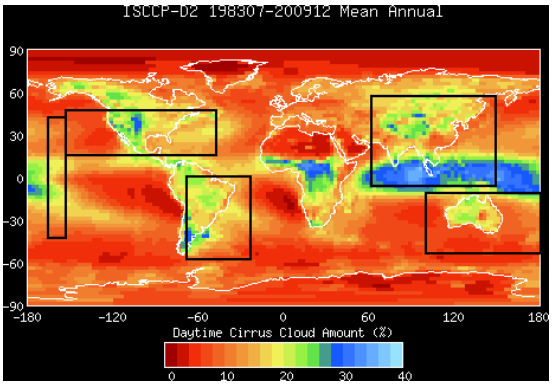

(b) Annual cirrus cloud amount.

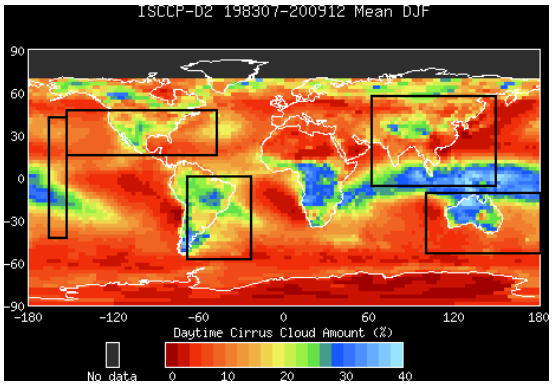

(c) Dec, Jan, Feb cirrus cloud amount.

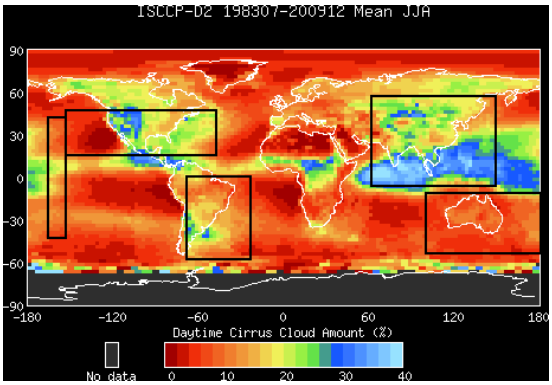

(d) Jun, Jul, Aug cirrus cloud amount.

Figure 3.24: World maps with cloud climatology with retrieval areas indicated, adapted from ISCCP-D2 dataset [Schiffer and Rossow, 1983], [Rossow and Schiffer, 1999].

4 Conclusions and Recommendations

The purpose of this study was to perform cloudy retrievals of XCO_2 on a larger scale and to analyse the data yield and the potentially increased spatial coverage over the oceans. To analyse the quality of the retrievals, a qualitative comparison is made with XCO_2 retrievals obtained from TCCON, clear-sky land and glint ocean measurements. Finally an qualitative analysis is done on the influence of different cloud climatologies on the retrieval behaviour

The analysis of the increase in coverage over the ocean was done by applying the cloudy retrieval method to GOSAT data and compare the results to glint retrievals. It has been shown that the amount of data from cloud retrievals is on average 2.4 times higher than glint retrievals, in areas where both methods can be applied. Furthermore, glint measurements are limited to low and middle latitudes, whereas cloud retrievals can be performed at all GOSAT measurement latitudes. Extrapolating the results gives an indication of the global data yield, which is approximately 2.5 times higher than the amount of successful clear-sky retrievals and approximately 8 times higher than the amount of glint retrievals per year. However, the quality of the data is poor with a scatter of the error with TCCON measurements of on average 4.23 ppm (1.13%), compared to 2.50 ppm (0.35%).

The comparison of the retrieval results with colocated TCCON measurements showed similar results in terms of amount of error scatter as [Schepers et al., 2016], where the retrievals from Oceania and North America show more robust statistics than the ones from East Asia. The comparison with colocated clear-sky and glint full physics retrievals show the same pattern, with an average error scatter of, respectively, 5.00 ppm (1.30%) and 5.03 ppm (1.30%) XCO_2.

The influence of cloud climatology on the retrieval quality was assessed by looking for correlations between ISCCP cloud data and the retrieval results. The relative high amount of successful retrievals and higher quality of successful retrievals over North-America and Oceania compared to East Asia could have been caused by a higher amount of low liquid clouds above those areas compared to East Asia. Another reason could be the larger amount of cirrus cloud, situated above South Asia. The seasonal dependency of the percentage of successful retrievals on the cirrus cloud seasonality is yet another indication.

Several recommendation can be made for further research on this topic. First of all, the cloud filter using the maximum LER value should be revised, which would decrease the amount of non-converging retrievals and thus save computational effort. This would make an analysis of the complete dataset of GOSAT and especially OCO-2 measurements more feasible. A more sophisticated cloud filter that would be able to distinguish undesired difficult cloud scenes from the low liquid clouds would further reduce the computation time and retrieval error.

Improvements of the quality of the retrievals could be made by implementing a cirrus cloud filter, based on current cirrus filters for clear-sky retrievals, such as [Guerlet et al., 2013] and [Taylor et al., 2016]. Further investigation into the influence of cloud climatology using a quantitative approach is necessary, using the dataset from ISCCP. Looking for correlations between this cloud dataset and a longer dataset of GOSAT, by using the CarbonTracker 2016 for the XCO_2 prior, will provide a solid ground for analysing this.

The influence of filling up the null-space by a priori CO_2 profiles on the retrieved XCO_2 should be analysed, in order to know how the error in CarbonTracker propagates into the retrieval. A comparison of colocated CarbonTracker and TCCON values could give an indication of the order of magnitude of the error.

Finally, the cloud retrieval in RemoTeC has to be revised in order to do retrievals for OCO-2 measurements, as the current setup is tailored for GOSAT retrievals.

Bibliography

[Alexe et al., 2015] Alexe, M., Bergamaschi, P., Segers, A., Detmers, R., Butz, A., Hasekamp, O., Guerlet, S., Parker, R., Boesch, H., Frankenberg, C., et al. (2015). Inverse modelling of CH 4 emissions for 2010–2011 using different satellite retrieval products from GOSAT and SCIAMACHY. *Atmospheric Chemistry and Physics*, 15(1):113–133.

[Blumenstock et al., 2014] Blumenstock, T., Hase, F., Schneider, M., Garcia, O., and Sepulveda, E. (2014). TCCON data from Izana (ES), Release GGG2014R0, TCCON data archive, hosted by CDIAC, doi: 10.14291/tccon. ggg2014. izana01. *R0/1149295*.

[Butz et al., 2011] Butz, A., Guerlet, S., Hasekamp, O., Schepers, D., Galli, A., Aben, I., Frankenberg, C., Hartmann, J.-M., Tran, H., Kuze, A., et al. (2011). Toward accurate CO2 and CH4 observations from GOSAT. *Geophysical Research Letters*, 38(14).

[De Mazière et al., 2014] De Mazière, M., Sha, M., Desmet, F., Hermans, C., Scolas, F., Kumps, N., Metzger, J., Duflot, V., and Cammas, J. (2014). TCCON data from Reunion Island (La Reunion), France, Release GGG2014R0, TCCON data archive, hosted by the Carbon Dioxide Information Analysis Center, Oak Ridge National Laboratory, Oak Ridge, Tennessee, USA. *Oak Ridge Natl. Lab., Oak Ridge, Tenn., doi*, 10.

[Deng et al., 2016] Deng, F., Jones, D., O'Dell, C. W., Nassar, R., and Parazoo, N. C. (2016). Combining GOSAT XCO2 observations over land and ocean to improve regional CO2 flux estimates. *Journal of Geophysical Research: Atmospheres*, 121(4):1896–1913.

[Eldering et al., 2017] Eldering, A., O'Dell, C. W., Wennberg, P. O., Crisp, D., Gunson, M. R., Viatte, C., Avis, C., Braverman, A., Castano, R., Chang, A., et al. (2017). The Orbiting Carbon Observatory-2: first 18 months of science data products. *Atmospheric Measurement Techniques*, 10(2):549.

[Griffith et al., 2014a] Griffith, D., Deutscher, N., Velazco, V., Wennberg, P., Yavin, Y., Aleks, G. K., Washenfelder, R., Toon, G., Blavier, J., Murphy, C., et al. (2014a). TCCON data from Darwin, Australia, Release GGG2014R0, TCCON data archive, hosted by the Carbon Dioxide Information Analysis Center, Oak Ridge National Laboratory, Oak Ridge, Tennessee, USA. *Oak Ridge Natl. Lab., Oak Ridge, Tenn., doi*, 10.

[Griffith et al., 2014b] Griffith, D., Velazco, V., Deutscher, N., Murphy, C., Jones, N., Wilson, S., Macatangay, R., Kettlewell, G., Buchholz, R., and Riggenbach, M. (2014b). TCCON data from Wollongong, Australia, Release GGG2014R0, TCCON data archive, hosted by the Carbon Dioxide Information Analysis Center, Oak Ridge National Laboratory, Oak Ridge, Tennessee, USA. *Oak Ridge Natl. Lab., Oak Ridge, Tenn., doi*, 10.

[Guerlet et al., 2013] Guerlet, S., Butz, A., Schepers, D., Basu, S., Hasekamp, O., Kuze, A., Yokota, T., Blavier, J.-F., Deutscher, N., Griffith, D. T., et al. (2013). Impact of aerosol and thin cirrus on retrieving and validating XCO2 from GOSAT shortwave infrared measurements. *Journal of Geophysical Research: Atmospheres*, 118(10):4887–4905.

[Kawakami et al., 2014] Kawakami, S., Ohyama, H., Arai, K., Okumura, H., Taura, C., Fukamachi, T., and Sakashita, M. (2014). TCCON data from Saga (JP), Release GGG2014R0, TCCON data archive, hosted by CDIAC, doi: 10.14291/tccon. ggg2014. saga01. *R0/1149283*.

[Kuze et al., 2009] Kuze, A., Suto, H., Nakajima, M., and Hamazaki, T. (2009). Thermal and near infrared sensor for carbon observation Fourier-transform spectrometer on the Greenhouse Gases Observing Satellite for greenhouse gases monitoring. *Applied optics*, 48(35):6716–6733.

[Miller et al., 2007] Miller, C., Crisp, D., DeCola, P., Olsen, S., Randerson, J. T., Michalak, A. M., Alkhaled, A., Rayner, P., Jacob, D. J., Suntharalingam, P., et al. (2007). Precision requirements for space-based data. *Journal of Geophysical Research: Atmospheres*, 112(D10).

[O'Dell and Feist, 2016] O'Dell, C. W. and Feist, D. G. (2016). Validation of TANSO-FTS/GOSAT XCO 2 and XCH 4 glint mode retrievals using TCCON data from near-ocean sites. *Atmospheric Measurement Techniques*, 9(3):1415.

[Ohyama et al., 2009] Ohyama, H., Morino, I., Nagahama, T., Machida, T., Suto, H., Oguma, H., Sawa, Y., Matsueda, H., Sugimoto, N., Nakane, H., et al. (2009). Column-averaged volume mixing ratio of CO2 measured with ground-based Fourier transform spectrometer at Tsukuba. *Journal of Geophysical Research: Atmospheres*, 114(D18).

[Peters et al., 2007] Peters, W., Jacobson, A. R., Sweeney, C., Andrews, A. E., Conway, T. J., Masarie, K., Miller, J. B., Bruhwiler, L. M., Pétron, G., Hirsch, A. I., et al. (2007). An atmospheric perspective on North American carbon dioxide exchange: CarbonTracker. *Proceedings of the National Academy of Sciences*, 104(48):18925–18930.

[Prentice et al., 2001] Prentice, I. C., Farquhar, G., Fasham, M., Goulden, M., Heimann, M., Jaramillo, V., Kheshgi, H., LeQuéré, C., Scholes, R., and Wallace, D. W. (2001). The carbon cycle and atmospheric carbon dioxide. Cambridge University Press.

[Rossow and Schiffer, 1999] Rossow, W. B. and Schiffer, R. A. (1999). Advances in understanding clouds from ISCCP. *Bulletin of the American Meteorological Society*, 80(11):2261–2287.

[Schepers, 2016] Schepers, D. (2016). Observing atmospheric methane from space.

[Schepers et al., 2014] Schepers, D., aan de Brugh, J., Hahne, P., Butz, A., Hasekamp, O., and Landgraf, J. (2014). LINTRAN v2. 0: A linearised vector radiative transfer model for efficient simulation of satellite-born nadir-viewing reflection measurements of cloudy atmospheres. *Journal of Quantitative Spectroscopy and Radiative Transfer*, 149:347–359.

[Schepers et al., 2016] Schepers, D., Butz, A., Hu, H., Hasekamp, O., Arnold, S., Schneider, M., Feist, D. G., Morino, I., Pollard, D., Aben, I., et al. (2016). Methane and carbon dioxide total column retrievals from cloudy GOSAT soundings over the oceans. *Journal of Geophysical Research: Atmospheres*, 121(9):5031–5050.

[Schiffer and Rossow, 1983] Schiffer, R. and Rossow, W. B. (1983). The International Satellite Cloud Climatology Project(ISCCP)-The first project of the World Climate Research Programme. *American Meteorological Society, Bulletin*, 64:779–784.

[Sherlock et al., 2014] Sherlock, V., Connor, B., Robinson, J., Shiona, H., Smale, D., and Pollard, D. (2014). TCCON data from Lauder. *New Zealand, 120HR, Release GGG2014R0, TCCON data archive, hosted by the Carbon Dioxide Information Analysis Center, Oak Ridge National Laboratory, Oak Ridge, Tennessee, USA, doi*, 10.

[Stocker, 2014] Stocker, T. (2014). *Climate change 2013: the physical science basis: Working Group I contribution to the Fifth assessment report of the Intergovernmental Panel on Climate Change*. Cambridge University Press.

[Taylor et al., 2016] Taylor, T. E., O'Dell, C. W., Partain, P. T., Cronk, H. Q., Nelson, R. R., Rosenthal, E. J., Chang, A. Y., Osterman, G. B., Pollock, R. H., and Gunson, M. R. (2016). Orbiting Carbon Observatory-2 (OCO-2) cloud screening algorithms: validation against collocated MODIS and CALIOP data. *Atmospheric Measurement Techniques*, 9(3):973.

[Wennberg et al., 2014a] Wennberg, P., Roehl, C., Wunch, D., Toon, G., Blavier, J., Washenfelder, R., Keppel Aleks, G., Allen, N., and Ayers, J. (2014a). TCCON data from Park Falls (US), Release GGG2014R0, TCCON data archive, hosted by CDIAC, doi: 10.14291/tccon. ggg2014. parkfalls01. *R0/1149161*.

[Wennberg et al., 2014b] Wennberg, P., Wunch, D., Roehl, C., Blavier, J., Toon, G., and Allen, N. (2014b). TCCON data from California Institute of Technology, Pasadena, California, USA, Release GGG2014R1. *TCCON Data Archive, Hosted by the Carbon Dioxide Inf. Anal. Center, Oak Ridge Nat. Lab., Oak Ridge, TN, USA*.